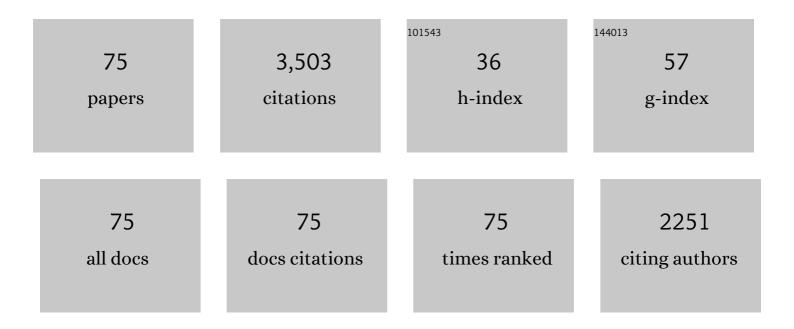
List of Publications by Year in descending order

Source: https://exaly.com/author-pdf/11805987/publications.pdf Version: 2024-02-01



#	Article	IF	CITATIONS
1	Based on graphene tunable dual-band terahertz metamaterial absorber with wide-angle. Optics Communications, 2018, 415, 194-201.	2.1	157
2	Bimetallic CoFe-MOF@Ti3C2Tx MXene derived composites for broadband microwave absorption. Chemical Engineering Journal, 2022, 431, 134007.	12.7	145
3	A polarization-insensitive and omnidirectional broadband terahertz metamaterial absorber based on coplanar multi-squares films. Optics and Laser Technology, 2013, 48, 415-421.	4.6	130
4	A photoexcited broadband switchable metamaterial absorber with polarization-insensitive and wide-angle absorption for terahertz waves. Optics Communications, 2016, 361, 41-46.	2.1	123
5	A novel two-layer honeycomb sandwich structure absorber with high-performance microwave absorption. Composites Part A: Applied Science and Manufacturing, 2019, 119, 1-7.	7.6	121
6	Infrared non-planar plasmonic perfect absorber for enhanced sensitive refractive index sensing. Optical Materials, 2016, 53, 195-200.	3.6	118
7	Hollow Beaded Fe ₃ C/N-Doped Carbon Fibers toward Broadband Microwave Absorption. ACS Applied Materials & Interfaces, 2022, 14, 3084-3094.	8.0	103
8	Giant asymmetric transmission of circular polarization in layer-by-layer chiral metamaterials. Applied Physics Letters, 2013, 103, .	3.3	93
9	Effects of aspect ratio and particle size on the microwave properties of Fe–Cr–Si–Al alloy flakes. Materials Science & Engineering A: Structural Materials: Properties, Microstructure and Processing, 2007, 466, 178-182.	5.6	90
10	Synthesis of yolk-shell structured carbonyl iron@void@nitrogen doped carbon for enhanced microwave absorption performance. Journal of Alloys and Compounds, 2020, 812, 152083.	5.5	88
11	Nickel/Nickel phosphide composite embedded in N-doped carbon with tunable electromagnetic properties toward high-efficiency microwave absorption. Composites Part A: Applied Science and Manufacturing, 2021, 140, 106141.	7.6	85
12	1D magnetic nitrogen doped carbon-based fibers derived from NiFe Prussian blue analogues embedded polyacrylonitrile via electrospinning with tunable microwave absorption. Composites Part B: Engineering, 2021, 224, 109161.	12.0	85
13	A photoexcited switchable perfect metamaterial absorber/reflector with polarization-independent and wide-angle for terahertz waves. Optical Materials, 2016, 62, 28-33.	3.6	84
14	Dual-band plasmonic perfect absorber based on all-metal nanostructure for refractive index sensing application. Materials Letters, 2018, 219, 123-126.	2.6	84
15	Design and characterization of one-dimensional photonic crystals based on ZnS/Ge for infrared-visible compatible stealth applications. Optical Materials, 2016, 62, 52-56.	3.6	83
16	An ultrathin transparent metamaterial polarization transformer based on a twist-split-ring resonator. Applied Physics A: Materials Science and Processing, 2013, 111, 209-215.	2.3	82
17	Triple narrow-band plasmonic perfect absorber for refractive index sensing applications of optical frequency. OSA Continuum, 2019, 2, 2113.	1.8	78
18	Ultra-Broadband Linear Polarization Conversion via Diode-Like Asymmetric Transmission with Composite Metamaterial for Terahertz Waves. Plasmonics, 2017, 12, 1113-1120.	3.4	77

#	Article	IF	CITATIONS
19	Dual and broadband terahertz metamaterial absorber based on a compact resonator structure. Optical Materials Express, 2018, 8, 3104.	3.0	77
20	Electromagnetic manifestation of chirality in layer-by-layer chiral metamaterials. Optics Express, 2013, 21, 5239.	3.4	68
21	Adjustable low frequency and broadband metamaterial absorber based on magnetic rubber plate and cross resonator. Journal of Applied Physics, 2014, 115, .	2.5	67
22	Design and realization of one-dimensional double hetero-structure photonic crystals for infrared-radar stealth-compatible materials applications. Journal of Applied Physics, 2014, 116, .	2.5	65
23	Circular polarization converters based on bi-layered asymmetrical split ring metamaterials. Applied Physics A: Materials Science and Processing, 2014, 116, 643-648.	2.3	65
24	Ultra-thin Low-Frequency Broadband Microwave Absorber Based on Magnetic Medium and Metamaterial. Journal of Electronic Materials, 2017, 46, 1293-1299.	2.2	62
25	Synergistic effect of silica coated porous rodlike nickel ferrite and multiwalled carbon nanotube with improved electromagnetic wave absorption performance. Journal of Alloys and Compounds, 2019, 802, 364-372.	5.5	60
26	Dual-band and high-efficiency circular polarization conversion via asymmetric transmission with anisotropic metamaterial in the terahertz region. Optical Materials Express, 2019, 9, 1365.	3.0	57
27	Multi-interfacial magnetic carbon nanotubes encapsulated hydrangea-like NiMo/MoC/N-doped carbon composites for efficient microwave absorption. Carbon, 2022, 196, 828-839.	10.3	54
28	Preparation and microwave absorption properties of metal magnetic micropowder-coated honeycomb sandwich structures. Smart Materials and Structures, 2007, 16, 1501-1505.	3.5	52
29	Magnetic properties of carbonyl iron fibers and their microwave absorbing characterization as the filer in polymer foams. Journal of Alloys and Compounds, 2008, 456, 452-455.	5.5	50
30	Preparation and microwave absorption properties of foam-based honeycomb sandwich structures. Europhysics Letters, 2009, 85, 58003.	2.0	49
31	Enhanced microwave absorption of multiferroic Co 2 Z hexaferrite–BaTiO 3 composites with tunable impedance matching. Journal of Alloys and Compounds, 2015, 643, 111-115.	5.5	46
32	Design of a wideband reflective linear polarization converter based on the ladder-shaped structure metasurface. Optik, 2017, 137, 148-155.	2.9	45
33	Fe/Fe ₃ O ₄ @N-Doped Carbon Hexagonal Plates Decorated with Ag Nanoparticles for Microwave Absorption. ACS Applied Nano Materials, 2019, 2, 7266-7278.	5.0	43
34	Electromagnetic properties of Fe55Ni45 fiber fabricated by magnetic-field-induced thermal decomposition. Materials Chemistry and Physics, 2005, 94, 408-411.	4.0	39
35	Metamaterial absorber and extending absorbance bandwidth based on multi-cross resonators. Applied Physics B: Lasers and Optics, 2013, 111, 483-488.	2.2	39
36	Effect of Particle Size and Concentration on Microwave-Absorbing Properties of CuxCo2-xY (x=0, 1) Hexaferrite Composites. Journal of the American Ceramic Society, 2006, 89, 1450-1452.	3.8	37

#	Article	IF	CITATIONS
37	Effective strategy for visible-infrared compatible camouflage: surface graphical one-dimensional photonic crystal. Optics Letters, 2018, 43, 5323.	3.3	36
38	Fe3O4 cladding enhanced magnetic natural resonance and microwave absorption properties of Fe0.65Co0.35 alloy flakes. Journal of Alloys and Compounds, 2015, 646, 345-350.	5.5	34
39	Synthesis and excellent microwave absorption properties of reduced graphene oxide/FeNi ₃ /Fe ₃ O ₄ composite. New Journal of Chemistry, 2016, 40, 6238-6243.	2.8	34
40	Optimization of two-layer electromagnetic wave absorbers composed of magnetic and dielectric materials in gigahertz frequency band. Journal of Applied Physics, 2005, 98, 084903.	2.5	33
41	Microwave properties of surface modified Fe–Co–Zr alloy flakes with mechanochemically synthesized polystyrene. Journal of Alloys and Compounds, 2009, 480, 761-764.	5.5	33
42	Dynamics of two coupled Bose-Einstein Condensate solitons in an optical lattice. Optics Express, 2006, 14, 3594.	3.4	30
43	ULTRABROADBAND DIODE-LIKE ASYMMETRIC TRANSMISSION AND HIGH-EFFICIENCY CROSS-POLARIZATION CONVERSION BASED ON COMPOSITE CHIRAL METAMATERIAL. Progress in Electromagnetics Research, 2017, 160, 89-101.	4.4	30
44	Construction of hollow core-shelled nitrogen-doped carbon-coated yttrium aluminum garnet composites toward efficient microwave absorption. Journal of Colloid and Interface Science, 2022, 622, 181-191.	9.4	30
45	Ultra-thin and polarization-independent phase gradient metasurface for high-efficiency spoof surface-plasmon-polariton coupling. Applied Physics Express, 2015, 8, 122001.	2.4	27
46	Ultrabroadband Metamaterial Absorber Based on Effectively Coupled Multilayer HIS Loaded Structure With Dallenbach Layer. IEEE Transactions on Microwave Theory and Techniques, 2022, 70, 232-238.	4.6	25
47	An ultra-thin dual-band phase-gradient metasurface using hybrid resonant structures for backward RCS reduction. Applied Physics B: Lasers and Optics, 2017, 123, 1.	2.2	23
48	Co-Evaluation of Reflection Loss and Surface Wave Attenuation for Magnetic Absorbing Material. IEEE Transactions on Antennas and Propagation, 2018, 66, 6057-6060.	5.1	23
49	Multi-layer composite structure covered polytetrafluoroethylene for visible-infrared-radar spectral Compatibility. Journal Physics D: Applied Physics, 2017, 50, 505108.	2.8	22
50	Preparation and microwave absorption properties of honeycomb core structures coated with composite absorber. AIP Advances, 2018, 8, .	1.3	22
51	Quasi-periodic photonic crystal Fabry–Perot optical filter based on Si/SiO ₂ for visible-laser spectral selectivity. Journal Physics D: Applied Physics, 2018, 51, 225103.	2.8	21
52	Perfect dual-band circular polarizer based on twisted split-ring structure asymmetric chiral metamaterial. Applied Optics, 2014, 53, 5763.	1.8	19
53	Monodomain Design and Permeability Study of High-Q-Factor NiCuZn Ferrites for Near-Field Communication Application. Journal of Electronic Materials, 2015, 44, 4367-4372.	2.2	19
54	Temperature characteristics of Ge/ZnS one-dimension photonic crystal for infrared camouflage. Optical Materials, 2021, 121, 111564.	3.6	18

4

#	Article	IF	CITATIONS
55	Bimetallic Oxalate Rod-Derived NiFe/Fe ₃ O ₄ @C Composites with Tunable Magneto-dielectric Properties for High-Performance Microwave Absorption. Journal of Physical Chemistry C, 2021, 125, 24540-24549.	3.1	18
56	Nanostructured Ge/ZnS Films for Multispectral Camouflage with Low Visibility and Low Thermal Emission. ACS Applied Nano Materials, 2022, 5, 5119-5127.	5.0	18
57	Synthesis of nitrogen-doped graphene wrapped SnO ₂ hollow spheres as high-performance microwave absorbers. RSC Advances, 2019, 9, 10745-10753.	3.6	17
58	Preparation and excellent electromagnetic absorption properties of dendritic structured Fe3O4@PANI composites. Journal of Alloys and Compounds, 2022, 891, 161922.	5.5	17
59	Electromagnetic properties of Fe-Si-Al/BaTiO3/Nd2Fe14B particulate composites at microwave frequencies. Journal of Applied Physics, 2014, 115, .	2.5	16
60	Crystal structure tailored microwave magnetodielectric effect in YbYFeO ceramics. Journal of Alloys and Compounds, 2017, 726, 1030-1039.	5.5	16
61	Enhancement on high-temperature microwave absorption properties of TiB2–MgO composites with multi-interfacial effects. Ceramics International, 2021, 47, 4475-4485.	4.8	16
62	Photo-excited switchable broadband linear polarization conversion via asymmetric transmission with complementary chiral metamaterial for terahertz waves. OSA Continuum, 2019, 2, 2391.	1.8	16
63	Enhanced Microwave Absorption Properties of Flexible Polymer Composite Based on Hexagonal NiCo2O4 Microplates and PVDF. Journal of Electronic Materials, 2016, 45, 4202-4207.	2.2	13
64	Enhanced Microwave Absorption and Surface Wave Attenuation Properties of Co0.5Ni0.5Fe2O4 Fibers/Reduced Graphene Oxide Composites. Materials, 2018, 11, 508.	2.9	13
65	Enhanced Microwave Absorption of SiO2-Coated Fe0.65Co0.35 Flakes at a Wide Frequency Band (1a€"18AGHz), Journal of Electronic Materials, 2016, 45, 3640-3645 Adaptive infrared camouflage based on quasi-photonic crystal with <mml:math< td=""><td>2.2</td><td>12</td></mml:math<>	2.2	12
66	xmlns:mml="http://www.w3.org/1998/Math/MathML" display="inline" id="d1e439" altimg="si5.svg"> <mml:mrow><mml:msub><mml:mrow><mml:mi mathvariant="normal">Ge</mml:mi </mml:mrow><mml:mrow><mml:mn>2</mml:mn></mml:mrow>mathvariant="normal">Sb</mml:msub></mml:mrow> <mml:mrow><mml:mn>2</mml:mn></mml:mrow> <td>ısub2.amml sub> < mml</td> <td>:msub><mml :msub><mml:< td=""></mml:<></mml </td>	ısub 2.a mml sub> < mml	:msub> <mml :msub><mml:< td=""></mml:<></mml
67	mathvariant="normal">Te <mml:mrow><mml:mn>5<. Optics Communications, A polarization independent phase gradient metasurface for spoof plasmon polaritons coupling. Journal of Optics (United Kingdom), 2016, 18, 025101.</mml:mn></mml:mrow>	2.2	10
68	Monodomain NiCuZn Ferrite With High Miniaturization Factor and Low Magnetic Loss at 200 MHz for Antenna Miniaturization. IEEE Transactions on Magnetics, 2017, 53, 1-5.	2.1	10
69	Dual-band resonance induced broadband low-frequency radar absorber based on electric ring resonator embedded magnetic absorbing materials. Journal of Electromagnetic Waves and Applications, 2021, 35, 801-812.	1.6	7
70	Enhanced spectra selectivity of solar absorber film with Ti/Si 3 N 4 photonic structures. Materials Letters, 2017, 201, 5-8.	2.6	6
71	Design and fabrication of energy efficient film based on one-dimensional photonic band gap structures. Journal of Alloys and Compounds, 2017, 697, 1-4.	5.5	5
72	Variational analysis of evolution for magnetostatic envelope bright soliton with higher-order dispersion. Journal of Magnetism and Magnetic Materials, 2007, 313, 122-126.	2.3	1

#	Article	IF	CITATIONS
73	Tunable Electromagnetic and Microwave Absorption Properties of Ba3Co2Fe24O41/P(VDF-TrFE) Composites. IEEE Transactions on Magnetics, 2016, 52, 1-4.	2.1	1
74	A novel miniaturized and wideband microstrip antenna based on metamaterials. , 2016, , .		0
75	Valid corollaries of polarization-separated color attributes for a multi-layer dielectric structure. Physica Scripta, 2019, 94, 115007.	2.5	0